Journal of Materials Chemistry A

Accepted Manuscript

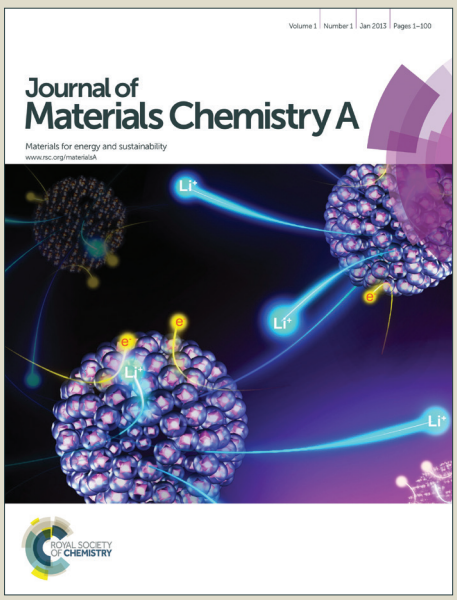

ROYAL SOCIETY OF CHEMISTRY

www.rsc.org/materialsA

Journal of Materials Chemistry A RSCPublishing

ARTICLE

From Biomass to High Performance Solar-Thermal and Electric-Thermal Energy Conversion and Storage Materials

Cite this: DOI: 10.1039/x0xx00000x

Received 00th January 2012,
Accepted 00th January 2012

DOI: 10.1039/x0xx00000x

www.rsc.org/

Yuanqing Li,*[a] Yarjan Abdul Samad,[a] Kyriaki Polychronopoulou,[b] Saeed M. Alhassan,[c] and Kin Liao*[a]

We have demonstrated that lightweight, highly electrical conductive, and three-dimensional (3D) carbon aerogels (CAs) can be produced *via* a hydrothermal carbonization and post pyrolysis process using various melons as raw materials. This two-steps process is a totally green and chemical-free synthetic method with cheap and ubiquitous biomass as the only raw material. These black-colored, high electrical conductive, and 3D structured CAs are ideal materials for energy conversion and storage. Paraffin wax was impregnated into the CA scaffold by vacuum infusion. The CA/wax composites obtained show excellent form-stable phase change behavior with a high melting enthalpy of 115.2 J/g. The CA/wax composite exhibits very high solar radiation absorption in the whole UV-Vis-NIR range, and 96% light can be absorbed by the phase-change composite and stored as thermal energy. With an electrical conductivity of 3.4 S/m, CA/wax composite can be triggered by low electric potential to perform energy storage and release, with an estimated electric-heat conversion efficiency of 71.4%. Furthermore, CA/wax composites have excellent thermal stability with stable melting-freezing enthalpy and excellent reversibility. With a combination of low-cost biomass as raw materials, green preparation process, low density, and excellent electrical conductivity, the 3D CAs are believed to have promising potential applications in many energy-related devices.

Introduction

A few centuries' industrialization and population boom have resulted in ever increasing demand for energy, environmental pollution through greenhouse gas emissions, and rise in fuel prices, all ensuing a pressing need for exploring renewable energy sources for a sustainable future.[1, 2] Solar energy is perhaps the most abundant and lasting renewable source available to replace fossil fuels. Conversion of solar power into thermal energy using phase change materials (PCMs) is particularly attractive, since they provide a high energy storage density and have the capacity to store energy as latent heat of fusion at a constant temperature.[3] Furthermore, electric-to-thermal energy conversion using PCMs has wide potential applications, such as converting off-peak electricity, usage in portable electronics and hybrid vehicles and other power systems.[3-6] Although PCMs are excellent materials for thermal energy storage, direct solar-to-thermal or electric-to-thermal energy conversion with PCMs has been hindered by several challenges: (a) the light-colored PCMs have low sunlight absorption, and consequently low solar harvest efficiency; (b) due to the inherently extremely low electrical conductivity of PCMs, it is impossible to covert electrical energy to thermal energy directly with PCMs; (c) molten PCMs need to be contained to prevent leakage.[3-12] Introducing dark materials, such as dye and carbon nanotubes (CNTs),[9-12] and electrical conductive filler, such as CNT and carbon fiber,[4, 6] have proven to enhance the solar-thermal and electrical-thermal conversion efficiency of organic PCMs, respectively. At the same time, the thermal conductivity of PCMs can be enhanced by incorporation high thermal conductive fillers such as CNT and graphene.[7, 13-15] However, a percolated conductive network and a stable composite structure especially at liquid state (above the melting point of PCMs) are difficult to realize with powder or fiber like fillers. Direct infiltration of organic PCMs into a carbon based aerogels, such as CNT and graphene aerogel composed of interconnected three-dimensional (3D) networks, has been demonstrated to be viable for achieving form-stable PCMs with simultaneous solar-to-thermal and electric-to-thermal energy conversion properties.[10, 16] However, the harmful and expensive precursors or complex equipment involved in CNT and graphene aerogel syntheses dramatically hamper their large-scale production for industry applications. Thus facile, economical, and environmentally friendly strategies to massively produce carbon-based aerogels are being sought.[17-20]

As a sustainable and renewable material, biomass can be directly transformed into carbon materials by a well-established hydrothermal carbonization (HTC) process under mild heating conditions.[21-23] This approach opens practical routes to the production of carbonous materials of varied structures, which have shown a variety of potential applications in energy storage, catalysis, bio-imaging, water purification, H_2 storage, and CO_2 capture.[24-30] Melons, such as winter melon (wax gourd), watermelon, and pumpkin, are typical natural material that are economical, sustainable, and contains more than 90% water and less than 10% polysaccharide biomass, making them promising raw material for fabrication of carbon based aerogels. We demonstrate that lightweight, highly electrical conductive, and 3D carbon aerogels (CAs) can be produced *via* a HTC and a post pyrolysis process using various melons as raw materials. This two-steps process is a totally green and chemical-free synthetic method with cheap and ubiquitous biomass as the only raw material. Then, CA/wax composites were fabricated by vacuum infusion of paraffin wax into the CA scaffold. Effective solar-to-thermal and electric-to-thermal energy conversion can be carried out with the composite PCM, and the thermal energy is stored in the PCMs by a form-stable phase transition. This novel CA/wax composite is believed to have broad potential application in energy harvest, conversion, and storage.

Experimental

Materials. Fresh winter melon (wax gourd), watermelon and pumpkin were obtained from local market. Paraffin wax with melting temperature 54-56^{o}C was purchased from Sigma-Aldrich Co. Ltd.

Preparation of carbon aerogels. First, the rind, soft pulp, and seeds from winter melon, water melon and pumpkin were removed. Then the flesh of winter melon, water melon (non-eatable peel part), and pumpkin was cut into appropriate shape and volume (around 20 cm^3), and placed into a Teflon-lined stainless steel autoclave. The autoclave was heated at 180^{o}C for 10 h under self-generated pressure in a closed system. Black or brown colored melon hydrogel monoliths were obtained after the hydrothermal reaction. The products were immersed in hot water (around 60^{o}C) for 2 days to remove the soluble impurities. The remaining melon aerogels were obtained by freeze drying. Finally, to fully convert the carbonaceous aerogel to carbon and improve the electrical conductivity, the dried aerogels were placed in a tube furnace and pyrolysed at 800^{o}C for 1 h in N_2 atmosphere.

Preparation of CA/wax composites. In order to make the CA/wax composite PCM, paraffin wax was melted at 100^{o}C, and the CAs prepared from winter melon were completely immersed into the liquid paraffin wax. Then the mixture was placed in a vacuum chamber for approximately 10 min for the CA to be infused with paraffin wax and to remove air bubbles. After the temperature of the mixture had cooled to room temperature, the black CA/wax composite sample was taken out from paraffin wax carefully, and the excessive paraffin wax adhered on the composite surface was removed by knife. The CA loading in the composite was determined by measuring the weight of the CA before infusion and of the composite after wax infusion.

Characterization. The morphology of CA and CA/wax composites was imaged by a FEI Quanta FEG 250 scanning electron microscopy (SEM). All opitcal pictures used in this paper were taken by a Canon digital camera (IXUS 70). X-ray diffraction (XRD) patterns of the samples were performed on a powder diffractometer (PANalytical, X'Pert3) with Cu Kα radiation (λ = 1.54056 Å). Porosimetry measurements were carried out using a high-resolution 3Flex Micromeritics adsorption instrument. The 3Flex Micromeritics was equipped with high-vacuum system, and three 0.1 Torr pressure transducers. The densities of CAs were calculated by measuring the weight and volume of the samples. The electrical conducitivity of CA were measured with a two-probe method using an ADM-930 Digital Multimeter (0.1Ω~40MΩ). The CA samples used for conductivity measurement were silver-pasted to minimize the contact resistance between the composites and the electrodes. The electrical conducitivity of CA/wax composites were measured using a four-point probe resistivity measurement system (RST 8, 4 Pro Tech). For all the density and electrical conductivity, more than 8 samples were tested, from which the average and standard deviation were calculated.

The optical properties of the paraffin wax and CA/wax composite were studied using a UV-vis-NIR spectrophotometer (Varian, Cary 5000) with integrating sphere. For the measurements, around 1g samples were filled in a hole of a sample holder and the surface smoothed. The reflection spectra were scanned in the range of 250-2500 nm with a 1-nm interval. The thermal properties of CA and CA/wax composites were investigated by a simultaneous thermogravimetry and differential scanning calorimetry (TG-DSC) (SDT 600, TA Instruments). The melting temperatures and latent heat of PCM were obtained at a heating rate of 2 ^{o}C/min. The weight loss and thermal stability of CA and CA/composite were obtained in the temperature range RT to 1000^{o}C at a heating rate of 20 ^{o}C/min.

Solar-to-thermal energy conversion and storage. 15 g wax and CA/wax composite were placed into 20 ml transparent glass beaker, respectively. Samples were directly illuminated by sun between 12:00 to 14:00 in October at Khalifa University, Abu Dhabi campus with an ambient temperature around 35^{o}C. The experiment was stopped until the temperature of CA/wax was stabilized or started to drop. Temperature evolution of the samples during the heating and natural cooling processes was measured by a thermometer (YC-747UD). Two thermal sensors were inserted into the wax and CA/wax composite respectively to monitor the temperature while data was collected by a data acquisition system with software Temp Monitor S2.

Electric-to-thermal energy conversion and storage. The prepared CA/wax composite was cut into a rectangular block with dimension of 50 mm (L) × 20 mm (W) × 15 mm (H). As shown in Figure S1, two side of the composite was connected to a laboratory DC power supply (Instek, GPS-3303) with two alumina sheets as electrodes. Each alumina sheet was attached onto the surface of composite by silver paste to ensure good electrical contact with CA/wax composite. A certain voltage (less than 30 V) was applied to the sample by the DC power supply for a certain time. Temperature evolution of the sample during the heating and natural cooling processes was measured by the same system as mentioned in solar-to-thermal energy conversion and storage measuring system. Electric-to-heat

conversion efficiency (η) can be estimated with the following equation:

$$\eta = \frac{m\Delta H}{UIt} \qquad (1)$$

where m and ΔH are, respectively, the weight (13.5 g) and enthalpy of the composite (376J/g), and U, I, and t are the voltage (15V), current (1.2 A) and applied time (395 s), respectively, during the electric-heat conversion process.

Results and discussion

As shown in Figure 1, the flesh of winter melon, watermelon, and pumpkin was cut into appropriate shape and size, and then the melon pieces were sealed in a hydrothermal autoclave and maintained at 180°C for 10 h. After the hydrothermal treatment, carbonaceous melon hydrogels (MH) that had maintained their original volume and shape but with large amount of water were obtained. Then the water from the MHs was removed by freeze drying to obtain melon aerogel (MA). As shown in Figure 2a, MA from winter melon exhibit porous structure with large sheet and fibrous structure of several hundreds of micron in size. Those sheets or fibres are indigestible dietary fibres of the plant. In addition, the MAs obtained show a dark brown colour, indicating low temperature hydrothermal treatment cannot fully convert the melon to carbon.

Figure 1. Schematic of preparation of CA and CA/wax composite: (1) and (2) winter melon, (3) winter melon hydrogel, (4) winter melon aerogel, (5) carbon aerogel, and (6) CA/wax composite.

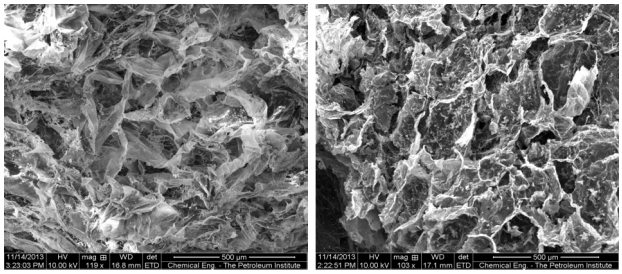

(a) (b)

Figure 2. SEM images of MA (a) and CA (b) from winter melon.

To obtain ideal CA, thermal analysis of melon aerogel was performed (Figure 3). Thermogravimetry (TG) curve of MA shows that most significant weight loss, more than 50%, occurs in the temperature range 250-600°C. Above 600°C, the mass of MA is almost unchanged, indicating the formation of CA. At the same time a high exothermic peak in the differential scanning calorimetry (DSC) curve is observed at around 400-550°C, which is likely to be associated with the conversion of MA to CA. Thus to fully convert MA to CA, the MAs are to be pyrolysed at 800°C for 1h under N_2 atmosphere. After pyrolysis, the volume of the CA from winter melon is only 23% of that of the MA, owing to evaporation of volatile organic species. The XRD pattern of CA (Figure 4) shows two broad peaks at around 24° and 44°, which are attributed to (002) and (101) reflections of graphite carbon, respectively.[31] The broad peaks indicate that the CA was an amorphous structure.

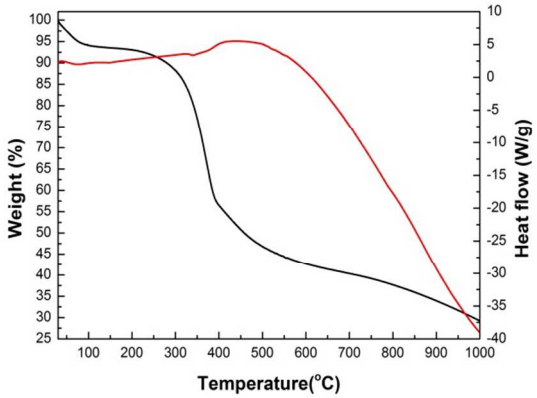

Figure 3. Thermal analysis of winter melon aerogel: TG and DSC curves.

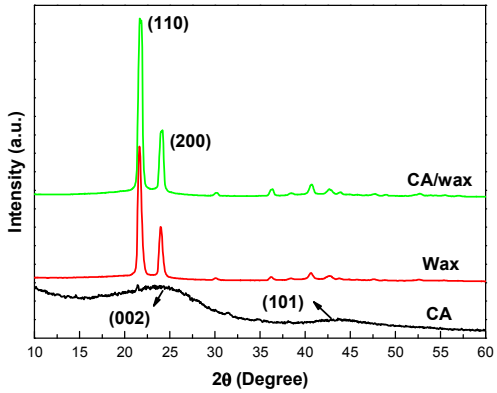

Figure 4. XRD patterns of CA (a), paraffin wax (b), and CA/wax composite.

The CAs from winter melon have very low density from 0.045 to 0.051 g/cm^3, the compositional difference of the melon samples leads to the slight variation of their density. The average density of CA (0.048 g/cm^3) is slightly higher than that of MA (0.035 g/cm^3). Compared with MA, CA shows a similar but contracted 3D structure with pore size around 200 μm (Figure 2b). The CAs from biomass possess an ultrahigh porosity of more than 95%, which is only slightly lower than those of CNT aerogels (99.5~99%) and graphene aerogels (99.5~98%).[10, 16-20] In addition, the BET surface area of CA from winter melon is 0.7 m^2/g only, which is much less than those of carbon aerogel from graphene and CNT due to large

sheet size. Despite their ultralight and high porosity, the CAs obtained exhibit a high electrical conductivity 6.5 S/m, which could have great potentials in energy conversion and electronic devices. CAs from water melon and pumpkin were also prepared (Figure 5), which exhibit well-connected 3D structures with pore size around 200 μm as well. The BET surface area of CA from water melon and pumpkin is 114 m^2/g and 5 m^2/g, respectively. Because watermelon contains a lot of sugar, which can transfer to carbon nanosphere via HTC process (Figure S2) and contribute to the high BET surface of CA from water melon. The density and conductivity of CAs from watermelon and pumpkin are similar to that of CA from winter melon (Table S1, supporting information).

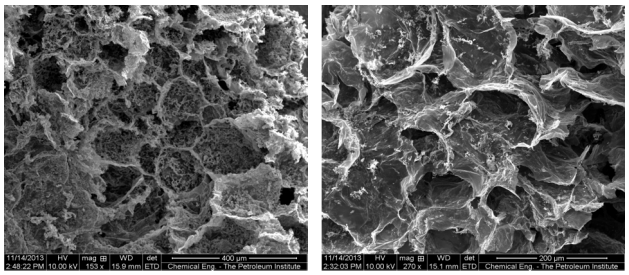

Figure 5. SEM images of CAs from watermelon (a) and pumpkin (b).

Black-coloured and with excellent electrical conductivity, these 3D structured CAs are good candidate to enhance solar-to-thermal conversion, electrical conductivity, and form-stable properties of organic PCMs. CA/wax composites were fabricated by vacuum infusion of liquid paraffin wax into the porous CAs (prepared from winter melon, because it is easier to obtain big samples from it). The high porosity of CA allows infiltration of paraffin wax at very high weight percentage (95 wt%). The crystallization of paraffin wax and CA/wax composite were investigated by XRD. In Figure 4, it is clear that paraffin wax has two sharp diffraction peaks at 2θ =21.6° and 2θ = 24.0°, which are attributed to the typical diffractions of (110) and (200) crystal planes of monoclinic paraffin, respectively.[32] The XRD pattern of the CA/wax composite display the same peaks as paraffin wax, no other peaks can be observed. The results suggest that the CA/wax composite has same crystallization as paraffin wax, and no new phase has been produced.

Figure 6 shows the heating-cooling behaviours of paraffin wax and CA/wax composite. Two transition peaks at heating process are clearly observed in both DSC curves, in which the sharp or main peak is attributed to the heterogeneously nucleated rotator-liquid transition which represents the solid-liquid phase change of the paraffin wax, and the minor peak corresponds to the solid-solid phase transition of paraffin.[7] The melting and freezing temperatures are determined to be 53.3 and 49.4°C for the pure wax, respectively, and 53.5 and 48.3°C for the composite, which are quite similar. The melting and freezing enthalpies measured from DSC curves are 122.3 and 134.1 J/g for the paraffin wax, respectively, and 115.2 and 126.9 J/g for the composite. Compared with paraffin wax, CA/wax composite exhibits only a partial loss of 5.8% in latent heat. During the melting and freezing process, absorption and release of thermal energy are dominated by paraffin wax, so high latent heat storage capacity in the composite PCM is the result of high content of the phase change material. On the basis of 95 wt% paraffin wax loading in CA/wax composite, the paraffin wax normalized melting enthalpy is 121.3 J/g, close to the value of paraffin wax (122.3 J/g).

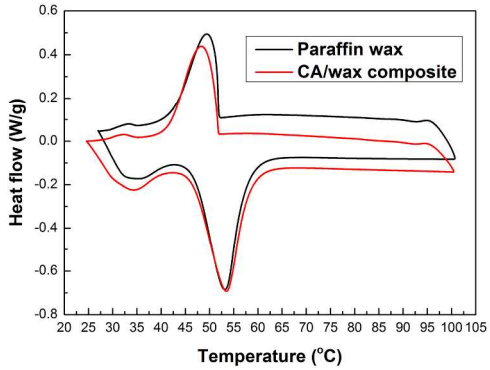

Figure 6. DSC curves of paraffin wax and CA/wax composite.

Leakage tests for paraffin wax above the melting temperature were carried out to investigate the form-stable property of the as-prepared CA/wax composite. Figure 7 shows the photographs of paraffin wax and CA/wax composite before and after being heated up to 100°C. After being heated to above its melting temperature, the paraffin wax was completely melted into liquid. The surface of the composite PCM was moistly, induced by the melting of wax, however, no liquid leakage from the composites was seen. It is seen from the fracture surface of CA/wax composite that CA scaffolds are wrapped by wax and the porous space is almost entirely filled up (Figure 8). Those micro-scaled pores of CA collectively suck in wax (enable by capillarity) and refrain it from spreading out during melting. Even after 20 cycles of melting-freezing phase change, the entire structure of the PCM composite remains stable without obvious leakage, indicating that the wax melting and freezing within the CA is reversible.

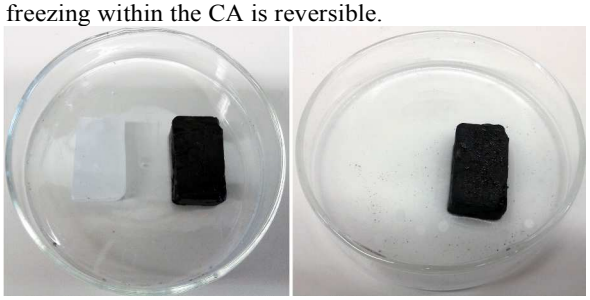

Figure 7. The form-stable comparison of paraffin wax and CA/wax composite: A) before heating, B) after heating over 100 °C.

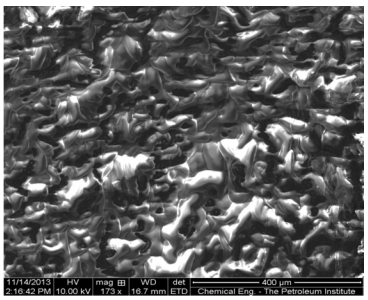

Figure 8. SEM image of the fracture surface of CA/wax composite.

The solar-to-thermal energy conversion behaviour of paraffin wax and CA/wax composite was investigated by placing the samples under sun light, and the temperature evolution inside the samples was recorded by a sensor and data collecting system, illustrated in Figure 9. Under the sun's radiation, the temperature of samples gradually rises as shown in Figure 10. Compared with paraffin wax, the temperature of CA/wax composite rises more rapidly. With the lapse of time, a melting plateau of the composite PCM appears between 48 and 54°C, indicating the solid-liquid phase change of wax. With further radiation, CA/wax composite sample reaches a stable state at around 70°C within 100 min. It should be mentioned that no thermal isolative protection was used for these samples, at low temperature only a small part of solar energy intake had dissipated to the surrounding. With an increase of temperature, the material-to-ambient heat dissipation also increases, until a temperature equilibrium was reached. At the same time, the stable temperature for pure wax is only 52°C, and no visible melting is seen due to the low solar-to-thermal conversion efficiency. The thermal release behaviour of PCMs and CA/wax is also shown in Figure 10. The temperature of CA/wax composite drops rapidly, immediately after being removed from sun radiation. Then a freezing plateau between 55.5 and 51°C that lasts for 34 min appears, indicating large amount of heat was released by CA/wax composite in the solidifying process. In contrast, no freezing plateau from paraffin wax is seen, due to the fact that the temperature of pure wax is below melting temperature. These results reveal that CA is an effective photon captor and molecular heater, that can absorb solar radiation, converting radiation into thermal energy, and store that energy in PCM.[9]

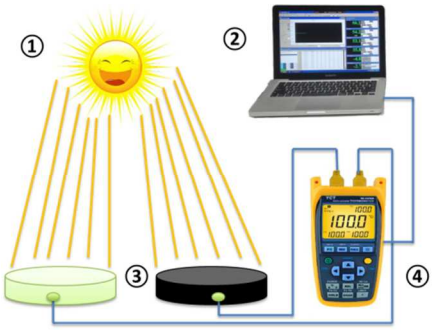

Figure 9. The schematic of solar to thermal energy conversion and storage measuring system: (1) Sun, (2) computer, (3) paraffin wax and CA/wax composite, and (4) thermometer.

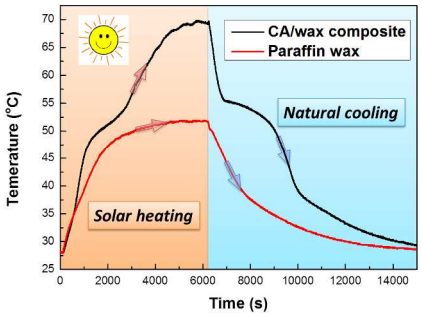

Figure 10. Solar-to-thermal conversion: temperature-time relationship of paraffin wax and CA/wax samples under sunlight radiation (12:00-13:30, October 21, 2013, Abu Dhabi, UAE with ambient temperature around 35°C).

To analyse the solar-to-thermal conversion efficiency of CA/wax composite, the UV-Vis-NIR absorption spectra of solid paraffin wax and CA/wax composite were obtained, shown in Figure 11. Paraffin wax only shows several absorption peaks at UV and NIR light range, no absorption peak is seen at visible light range (400~800 nm). The high background adsorption at visible light range is induced by the scattering of paraffin crystalline. However, the CA/wax composite exhibits total absorption characteristic in the whole UV-Vis-NIR range. These results agree well with the appearances of paraffin wax (white coloured) and CA/wax composite (black coloured). The black CA scaffold with porous structure behaves as a blackbody due to effective light scattering and trapping, and enhances photo absorption and in turn imparting thermal energy into the wax in the composites.[10] The average absorption of CA/wax composite over 200-2500 nm is close to 1.4, the calculated reflection is only 4%. Thus 96% solar radiation can be absorbed by PCM composite and stored as thermal energy.

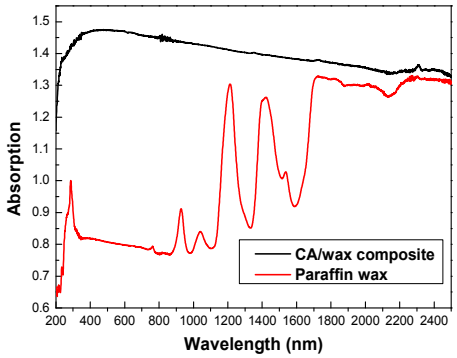

Figure 11. UV-Vis-NIR absorption spectrum of solid paraffin wax and CA/wax composite.

It is well known that paraffin wax is an excellent insulator with a conductivity of around 10^{-14} S/m. It is impossible to covert electric to thermal energy directly with paraffin wax. On the other hand, the electrical conductivity of CA/wax composite measured by four-probe method is 3.4 S/m, a 14-order-of-magnitude advantage over paraffin wax. Due to moderate electrical resistance, CA/wax composite can be triggered by low electric potential to perform energy storage and release. Figure 12 shows the temperature evolution of CA/wax composite under 15 V with a current of 1.2 A. Similar with the solar-to-thermal conversion, the temperature of CA/wax composite increases rapidly during the first two minutes, then reaches the melting plateau between 50 to 55°C, which lasts for 2 min before the wax is totally melted. After that, the temperature rises sharply again, and reaches 100°C within 6.5 min. After turning off the power supply, a freezing plateau that lasts for about 20 min is seen at 55-45°C, where the thermal energy stored during the melting process is released. When a current passes through the composite, Joule heat is generated by the resistance of carbon aerogel and also by the contact resistance in the network. The main heat transfer mechanism involves solid-to-solid heat conduction at the wax-carbon aerogel interface.[10] The electric-to-heat conversion efficiency, estimated by the ratio of heat stored in CA/wax composite and the applied electrical energy during the heating process, is 71.4%. Considering that the sample was exposed to surrounding without insulation, the real conversion efficiency should be even higher. Previous studies show that if a PCM

sample was well insulated, electric input can almost totally converted into heat and stored.[4]

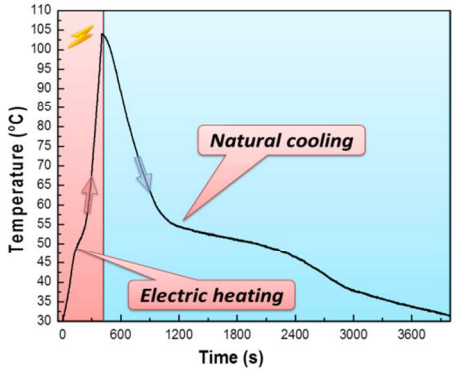

Figure 12. Electric-to-thermal conversion: temperature-time relationship of 12 g /Wax under 15 V，with 1.2 A current.

One of the main issues in PCM is the thermal stability after a long-term usage. Therefore, thermal, solar-thermal, and electric-thermal aging tests were performed to study the thermal reliabilities of CA/wax composites. After 20 cycles, no obvious changing can be seen from the DSC curves of CA/wax composites. The enthalpy of melting and freezing and peak temperature of heating and cooling is also quite similar (Figure 13 and Table S2, Supporting Information). The stable phase change performance and excellent reversibility of CA/wax composite are attributed to the CA scaffold, which can keep the structure intact with form-stable phase change processes.

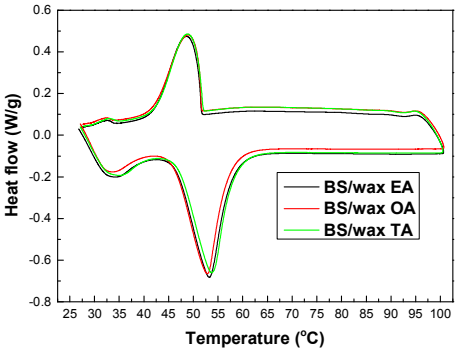

Figure 13. DSC curves of /wax composites after 20 electrical, optical, and thermal heating-cooling cycles.

Conclusions

In sum, CA samples from biomass were prepared via a HTC-post pyrolysis process. CAs prepared from winter melon showed a low density 0.048 g/cm^3 and excellent electrical conductivity of 6.5 S/m. Paraffin wax was impregnated into the CA scaffold by vacuum infusion. The CA/wax composites obtained show excellent form-stable phase change behavior with a high melting enthalpy of 115.2 J/g. The CA/wax composite exhibits very high solar radiation adsorption in the whole UV-Vis-NIR range, and 96% light can be absorbed by PCM composite and stored as thermal energy. With an electrical conductivity of 3.4 S/m, CA/wax composite can be triggered by low electric potential to perform energy storage and release, the estimated electric-to-heat conversion efficiency is 71.4%. Furthermore, CA/wax composites have excellent thermal stability with stable melting-freezing enthalpy and excellent reversibility. With a combination of low-cost biomass as raw materials, green preparation process, low density, and excellent electrical conductivity, the 3D CAs is believed to have promising potential applications in many energy-related devices.

Acknowledgements

The authors are grateful to the financial support by Khalifa University Internal Research Funds (No. 210008 and No. 210038).

Notes and references

[a] Aerospace Engineering Department, Khalifa University of Science, Technology, & Research, Abu Dhabi 127788, United Arab Emirates. Email: yqli@mail.ipc.ac.cn; kin.liao@kustar.ac.ae;
F : +971-(0)2-4472442.
[b] Mechanical Engineering Department, Khalifa University of Science, Technology, & Research, Abu Dhabi 127788, United Arab Emirates.
[c] Department of Chemical Engineering, The Petroleum Institute, Abu Dhabi 2533, United Arab Emirates.
Electronic Supplementary Information (ESI) available: [details of any supplementary information available should be included here]. See DOI: 10.1039/b000000x/

1. V. V. Tyagi, N. L. Panwar, N. A. Rahim and R. Kothari, *Renewable & Sustainable Energy Reviews*, 2012, **16**, 2289-2303.
2. D. Zhou, C. Y. Zhao and Y. Tian, *Applied Energy*, 2012, **92**, 593-605.
3. A. Sharma, V. V. Tyagi, C. R. Chen and D. Buddhi, *Renewable & Sustainable Energy Reviews*, 2009, **13**, 318-345.
4. K. Zhang, B. G. Han and X. Yu, *Energy Conversion and Management*, 2012, **64**, 62-67.
5. A. M. Khudhair and M. M. Farid, *Energy Conversion and Management*, 2004, **45**, 263-275.
6. Z. Liu, R. Zou, Z. Lin, X. Gui, R. Chen, J. Lin, Y. Shang and A. Cao, *Nano Lett.*, 2013, **13**, 4028-4035.
7. M. Mehrali, S. T. Latibari, H. S. C. Metselaar and M. Silakhori, *Energy Conversion and Management*, 2013, **67**, 275-282.
8. B. X. Li, T. X. Liu, L. Y. Hu, Y. F. Wang and S. B. Nie, *Chemical Engineering Journal*, 2013, **215**, 819-826.
9. Y. Wang, B. Tang and S. Zhang, *Adv Funct Mater*, 2013, **23**, 4354-4360.
10. L. J. Chen, R. Q. Zou, W. Xia, Z. P. Liu, Y. Y. Shang, J. L. Zhu, Y. X. Wang, J. H. Lin, D. G. Xia and A. Y. Cao, *ACS Nano*, 2012, **6**, 10884-10892.
11. Y. Wang, B. Tang and S. Zhang, *Journal of Materials Chemistry*, 2012, **22**, 18145-18150.
12. B. Tang, Y. Wang, M. Qiu and S. Zhang, *Solar Energy Materials and Solar Cells*, 2014, **123**, 7-12
13. S. Harish, K. Ishikawa, S. Chiashi, J. Shiomi and S. Maruyama, *Journal of Physical Chemistry C*, 2013, **117**, 15409-15413.
14. S. N. Schiffres, S. Harish, S. Maruyama, J. Shiomi and J. A. Malen, *ACS Nano*, 2013, **7**, 11183-11189.

15. L. W. Fan, X. Fang, X. Wang, Y. Zeng, Y. Q. Xiao, Z. T. Yu, X. Xu, Y. C. Hu and K. F. Cen, *Applied Energy*, 2013, **110**, 163-172.
16. Y. Zhong, M. Zhou, F. Huang, T. Lin and D. Wan, *Solar EnergyMaterials&SolarCells*, 2013, **113**, 195–200.
17. X. C. Gui, J. Q. Wei, K. L. Wang, A. Y. Cao, H. W. Zhu, Y. Jia, Q. K. Shu and D. H. Wu, *Adv. Mater.*, 2010, **22**, 617-+.
18. P. M. Sudeep, T. N. Narayanan, A. Ganesan, M. M. Shaijumon, H. Yang, S. Ozden, P. K. Patra, M. Pasquali, R. Vajtai, S. Ganguli, A. K. Roy, M. R. Anantharaman and P. M. Ajayan, *ACS Nano*, 2013, **7**, 7034-7040.
19. Z. P. Chen, W. C. Ren, L. B. Gao, B. L. Liu, S. F. Pei and H. M. Cheng, *Nature Materials*, 2011, **10**, 424-428.
20. Z. Y. Wu, C. Li, H. W. Liang, J. F. Chen and S. H. Yu, *Angewandte Chemie-International Edition*, 2013, **52**, 2925-2929.
21. M. M. Titirici, A. Thomas, S. H. Yu, J. O. Muller and M. Antonietti, *Chemistry of Materials*, 2007, **19**, 4205-4212.
22. B. Hu, K. Wang, L. H. Wu, S. H. Yu, M. Antonietti and M. M. Titirici, *Adv. Mater.*, 2010, **22**, 813-828.
23. R. J. White, V. Budarin, R. Luque, J. H. Clark and D. J. Macquarrie, *Chemical Society Reviews*, 2009, **38**, 3401-3418.
24. X. L. Wu, T. Wen, H. L. Guo, S. B. Yang, X. K. Wang and A. W. Xu, *ACS Nano*, 2013, **7**, 3589-3597.
25. L. Roldan, I. Santos, S. Armenise, J. M. Fraile and E. Garcia-Bordeje, *Carbon*, 2012, **50**, 1363-1372.
26. H. L. Wang, Z. Li, J. K. Tak, C. M. B. Holt, X. H. Tan, Z. W. Xu, B. S. Amirkhiz, D. Hayfield, A. Anyia, T. Stephenson and D. Mitlin, *Carbon*, 2013, **57**, 317-328.
27. W. Li, Z. H. Zhang, B. A. Kong, S. S. Feng, J. X. Wang, L. Z. Wang, J. P. Yang, F. Zhang, P. Y. Wu and D. Y. Zhao, *Angewandte Chemie-International Edition*, 2013, **52**, 8151-8155.
28. M. Sevilla and A. B. Fuertes, *Energy & Environmental Science*, 2011, **4**, 1765-1771.
29. M. Sevilla, A. B. Fuertes and R. Mokaya, *Energy & Environmental Science*, 2011, **4**, 1400-1410.
30. L. F. Chen, H. W. Lang, Y. Lu, C. H. Cui and S. H. Yu, *Langmuir*, 2011, **27**, 8998-9004.
31. X. Wang, X. Wang, L. Liu, L. Yi, C. Hu, X. Zhang and W. Yi, *Synthetic Metals*, 2011, **161**, 1725-1730.
32. B. Li, T. Liu, L. Hu, Y. Wang and L. Gao, *Acs Sustainable Chemistry & Engineering*, 2013, **1**, 374-380.